Inorg. Chem. **2003**, *42*, 8417–8429

Bridging Fluorides and Hard/Soft Mismatch in d^6 and d^8 Complexes: The Case of $[Tl(\mu\text{-}F)_3Ru(PPh_3)_3]$

Claus Becker, Iris Kieltsch, Diego Broggini,† and Antonio Mezzetti*

Department of Chemistry and Applied Biosciences, Swiss Federal Institute of Technology, ETH Hönggerberg, CH-8093 Zürich, Switzerland

Received July 28, 2003

$[RuCl_2(PPh_3)_3]$ reacts with thallium(I) fluoride to give either $[Tl(\mu\text{-}F)_3Ru(PPh_3)_3]$ (**1**) or $[Tl(\mu_3\text{-}F)(\mu_2\text{-}Cl)_2Ru_2(\mu_2\text{-}Cl)(\mu_2\text{-}F)(PPh_3)_4]$ (**2**) depending on the excess of TlF used. Both **1** and **2** were fully characterized, including X-ray structure determinations. Complex **1** reacts with dihydrogen to form the known ruthenium hydride complex $[Ru(H)_2(H_2)(PPh_3)_3]$ upon hydrogenolysis of the Ru–F bond. The reaction of **1** with activated alkyl bromides (R–Br) gives the corresponding alkyl fluorides and the trinuclear complex $[Tl(\mu_3\text{-}F)(\mu_2\text{-}F)(\mu_2\text{-}X)Ru_2(\mu_2\text{-}Br)(\mu_2\text{-}F)(PPh_3)_4]$ (X = Br, F) (**3**), whose structure closely resembles that of **2**. However, **1** is not active as catalyst for the nucleophilic fluorination of R–Br in the presence of thallium fluoride. The effect of the bridging coordination mode of fluoride on the Ru–F bond is discussed in terms of the HSAB principle, which suggests a more general model for predicting the stability of d^6 and d^8 complexes containing hard ligands (such as fluoro, oxo, and amido).

Introduction

In contrast to the large number of known ruthenium chloro complexes, there are relatively few literature reports concerning fluoro complexes of ruthenium(II).[1,2] In general, fluoro complexes of late transition metals are interesting both from a conceptual viewpoint (as examples of a combination of a "soft" late transition metal with a "hard" ligand) and as potential catalysts in organic transformations.[3] In the discussions of the properties of d^6 and d^8 fluoro complexes, there has been increasing consensus that fluoride acts as a stronger π-donor toward the metal than the heavier halides.[1,4−6] Also, as all orbitals with π-symmetry in d^6 and d^8 metals are filled, the 4-electron filled/filled $p\pi/d\pi$ repulsion discussed by Mayer[7] and Caulton[4] has been considered to play a pivotal role in these complexes. In an alternative approach, we have recently suggested[8] that the structure and reactivity of low-valent fluoro complexes of late transition metals is dominated by the ionic character of the M−F bond, which is an effect of the high electronegativity of fluorine. In fact, d^6 and d^8 fluoro complexes are generally labile and highly reactive toward nucleophiles, unless some kind of stabilizing interaction is operative.

Our tentative explanation was that all factors that enhance the electronegativity of the metal in the complex decrease the electronegativity difference between M and F and stabilize the M−F bond. This, admittedly very simplistic, concept is based on Pauling's electronegativity considerations and accounts for the observation that stable d^6 and d^8 fluoro complexes can be obtained by using strong π-accepting coligands that deplete the electron density at the metal. Examples are $[MF_2(CO)_2(PPh_3)_2]$ (M = Ru or Os)[9] and $[RuH(F)(CO)(PR_3)_2]$.[4b,10] Along the same lines, we have suggested[8] that the electron deficient nature of the metal stabilizes the M−F bond of 16-electron, π-stabilized[11] complexes such as $[IrH_2F(PBu^t_2Ph)_2]$[12] and $[RuF(dppp)_2]^+$

* To whom correspondence should be addressed. E-mail: mezzetti@inorg.chem.ethz.ch.
† X-ray structures.

(1) Doherty, N. M.; Hoffman, N. W. *Chem. Rev.* **1991**, *91*, 553.
(2) Murphy, E. F.; Murugavel, R.; Roesky, W. W. *Chem. Rev.* **1997**, *97*, 3425.
(3) Pagenkopf, B. L.; Carreira, E. M. *Chem. Eur. J.* **1999**, *5*, 3437.
(4) (a) Caulton, K. G. *New J. Chem.* **1994**, *18*, 25. (b) Poulton, J. T.; Sigalas, M. P.; Folting, K.; Streib, W. E.; Eisenstein, O.; Caulton, K. G. *Inorg. Chem.* **1994**, *33*, 1476.
(5) Grushin, V. V. *Chem. Eur. J.* **2002**, *8*, 1006.
(6) Fagnou, K.; Lautens, M. *Angew. Chem., Int. Ed.* **2002**, *41*, 26.
(7) Mayer, J. M. *Comments Inorg. Chem.* **1988**, *8*, 125.
(8) Mezzetti, A.; Becker, C. *Helv. Chim. Acta* **2002**, *85*, 2686.
(9) (a) Brewer, S. A.; Brisdon, A. K.; Holloway, J. H.; Hope, E. G.; Peck, L. A.; Watson, P. G. *J. Chem. Soc., Dalton Trans.* **1995**, 1073. See also: (b) Smith, G.; Cole-Hamilton, D. J.; Gregory, A. C.; Goodman, N. G. *Polyhedron* **1982**, *1*, 97.
(10) Poulton, J. T.; Sigalas, M. P.; Eisenstein, O.; Caulton, K. G. *Inorg. Chem.* **1993**, *32*, 5490.
(11) (a) Rachidi, I. E.; Eisenstein, O.; Jean, Y. *New. J. Chem.* **1990**, *14*, 671. (b) Riehl, J. F.; Jean, Y.; Eisenstein, O.; Pélissier, M. *Organometallics* **1992**, *11*, 729.
(12) Cooper, A. C.; Caulton, K. G: *Inorg. Chim. Acta* **1996**, *251*, 41.

10.1021/ic034888e CCC: $25.00
Published on Web 10/30/2003

(dppp = 1,3-bis(diphenylphosphino)propane).[13] The latter species is Lewis acidic because of the overall positive charge and the coordinative unsaturation of ruthenium.

Owing to its Lewis acidity, $[RuF(dppp)_2]^+$, which was prepared by reaction of $[RuCl(dppp)_2]^+$ with TlF,[13] is an active fluorinating agent of alkyl halides R−X (R = Cl, Br, or I) both as a stoichiometric reagent and as catalyst in combination with thallium(I) fluoride.[14] With the less bulky ligand 1,2-bis(diphenylphosphino)ethane (dppe), the reaction of $[RuCl(dppe)_2]^+$ with TlF yields the Ru−F−Tl bridged species $[Tl(\mu\text{-}F)_2Ru(dppe)_2]^+$ instead of the five-coordinate species $[RuF(dppe)_2]^+$.[14]

In our screening of five-coordinate, 16-electron fluoro complexes that might catalyze fluoride-transfer reactions, we targeted the preparation of the yet unknown difluoro complex $[RuF_2(PPh_3)_3]$. The corresponding complexes $[RuX_2(PPh_3)_n]$ (X = H, Cl, Br; n = 3, 4) catalyze a plethora of reactions[15] and act as precursors for the synthesis of other ruthenium complexes. As described below, the well-established strategy based on the fluorination of chloro complexes of ruthenium(II) with thallium(I) fluoride yielded, instead, the title compound $[Tl(\mu\text{-}F)_3Ru(PPh_3)_3]$ (**1**), which is a formal TlF adduct of the target complex $[RuF_2(PPh_3)_3]$.

The isolation of **1**, as well as Perutz's report of the fluoro-bridged binuclear cation $[Ru_2(\mu\text{-}F)_3(PEt_3)_6]^+$,[16] prompted us to reassess our ideas concerning the M−F bonding in fluoro complexes of late transition metals and to develop a general model that could explain both metal-centered (push−pull interactions and π-stabilization) and ligand-based factors, and in particular the role that the coordination mode of the fluoro ligand (terminal vs bridging) plays in the stabilization of d^6 and d^8 fluoro complexes. The ultimate goal is to develop a general understanding of the factors that determine the stability of d^6 and d^8 complexes containing hard ligands, such as fluoro, oxo, and amido.[17]

Experimental Section

General Methods. All operations were carried out under purified nitrogen in a glovebox by using Teflon reaction vessels and distilled solvents. All reagents and solvents were Fluka puriss. grade or had comparable purity. Dichlorotris(triphenylphosphine)ruthenium(II) was prepared according to literature procedures.[18] NMR spectra were recorded on Bruker Avance 250 and 300 spectrometers. Chemical shifts δ are in ppm relative to internal $SiMe_4$ (^{1}H), to external 85% H_3PO_4 (^{31}P), and to external $CFCl_3$ (^{19}F). NMR spectra were run at room temperature (unless otherwise stated) and were simulated with Swan-MR.[19] Elemental analyses were measured by the analytical service of the chemistry department of the ETH Zürich.

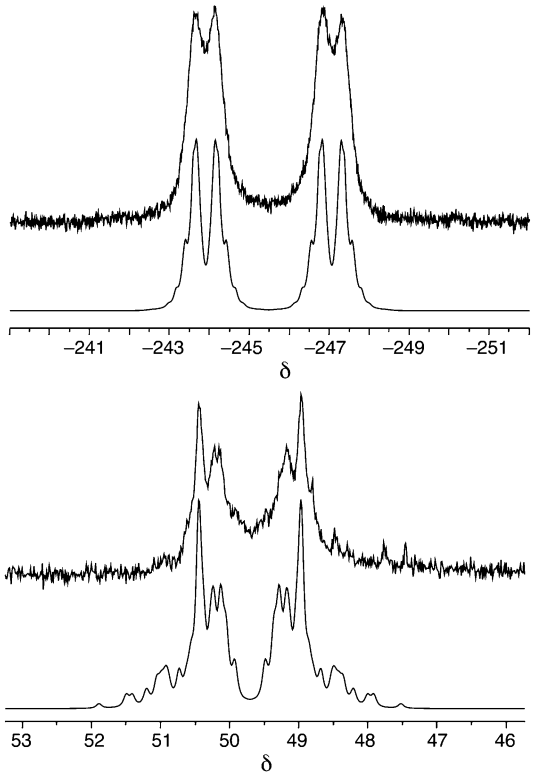

Figure 1. Experimental and simulated ^{19}F (upper) and ^{31}P (lower) NMR spectra of **1**.

Reaction of $[RuCl_2(PPh_3)_3]$ with TlF. $[RuCl_2(PPh_3)_3]$ (500 mg, 521 μmol) and thallium fluoride (350 mg, 1.6 mmol, 3 equiv) were suspended in dichloromethane (8 mL) in a Teflon reaction vessel in a glovebox and stirred at room temperature for 28 h. Then, the reaction mixture was filtered through a microfilter to remove the precipitated thallium salts, and the solvent was evaporated affording a dark red-brown solid. Crystals of $[Tl(\mu\text{-}F)_3Ru(PPh_3)_3]$ (**1**) and $[Tl(\mu_3\text{-}F)(\mu_2\text{-}Cl)_2Ru_2(\mu_2\text{-}Cl)(\mu_2\text{-}F)(PPh_3)_4]$ (**2**) were isolated from a mixed batch of yellow (**1**) and red (**2**) crystals obtained by slow diffusion of pentane into a $CDCl_3$ solution of the dark red-brown solid.

$[Tl(\mu\text{-}F)_3Ru(PPh_3)_3]$ (1). $[RuCl_2(PPh_3)_3]$ (2.00 g, 2.07 mmol), thallium fluoride (2.23 g, 10 mmol), and triphenylphosphine (2.63 g, 10 mmol) were suspended in dichloromethane (11 mL) in a Teflon reaction vessel in a glovebox and stirred at room temperature for 20 h. Then, the reaction mixture was filtered through a microfilter to remove the precipitated thallium salts, and the solvent was evaporated. The orange residue was recrystallized from dichloromethane/pentane and dried in a vacuum to give **2** as a yellow powder (1.45 g, 1.25 mmol, 60%). ^{31}P{^{1}H} NMR (CD_2Cl_2, 121 MHz), T = 25 °C: δ 49.5 (br s, 3 P). At −20 °C (Figure 1): δ 49.5 (MM′M″ part of AA′A″MM′M″X spin system, $J_{P,P'}$ = −26.6, $J_{P,F}$ = +201.4, $J_{P,F'}$ = −11.0, $J_{P,F''}$ = −10.4, $J_{Tl,P}$ = +3.0, 3 P). ^{19}F NMR (CD_2Cl_2, 282 MHz), T = 25 °C: δ −251 (br). At T = −60 °C: δ −251 (AA′A″ part of an AA′A″MM′M″X spin system, $J_{F,F'}$ = −100.0, $J_{Tl,F}$ = +890.3, 3 F). Anal. Calcd for $C_{54}H_{45}F_3P_3RuTl$: C, 56.43; H, 3.95, P, 8.08. Found: C, 56.42; H, 4.23; P, 8.05.

$[Tl(\mu_3\text{-}F)(\mu_2\text{-}Cl)_2Ru_2(\mu_2\text{-}Cl)(\mu_2\text{-}F)(PPh_3)_4]$ (2). $[RuCl_2(PPh_3)_3]$ (250 mg, 260 μmol) and thallium fluoride (29 mg, 130 μmol, 0.5 equiv) were suspended in dichloromethane (5 mL) in a Teflon reaction vessel in a glovebox and stirred at room temperature for 20 h. Then, the reaction mixture was filtered through a microfilter to remove the precipitated thallium salts yielding a dark red solution,

(13) (a) Barthazy, P.; Hintermann, L.; Stoop, R. M.; Woerle, M.; Mezzetti, A.; Togni, A. *Helv. Chim. Acta* **1999**, *82*, 2448. (b) Barthazy, P.; Stoop, R. M.; Woerle, M.; Togni, A.; Mezzetti, A. *Organometallics* **2000**, *19*, 2844.
(14) Barthazy, P.; Togni, A.; Mezzetti, A. *Organometallics* **2001**, *20*, 3472.
(15) Naota, T.; Takaya, H.; Murahashi, S. I. *Chem. Rev.* **1998**, *98*, 2599.
(16) Jasim, N. A.; Perutz, R. N.; Archibald, S. J. *J. Chem. Soc., Dalton Trans.* **2003**, 2184.
(17) Holland, P. L.; Andersen, R. A.; Bergman, R. G. *Comments Inorg. Chem.* **1999**, *21*, 115.
(18) Hallman, P. S.; Stephenson, T. A.; Wilkinson, G. *Inorg. Synth.* **1970**, *12*, 237.
(19) Balacco, G. *J. Chem. Inf. Comput. Sci.* **1994**, *34*, 1235.

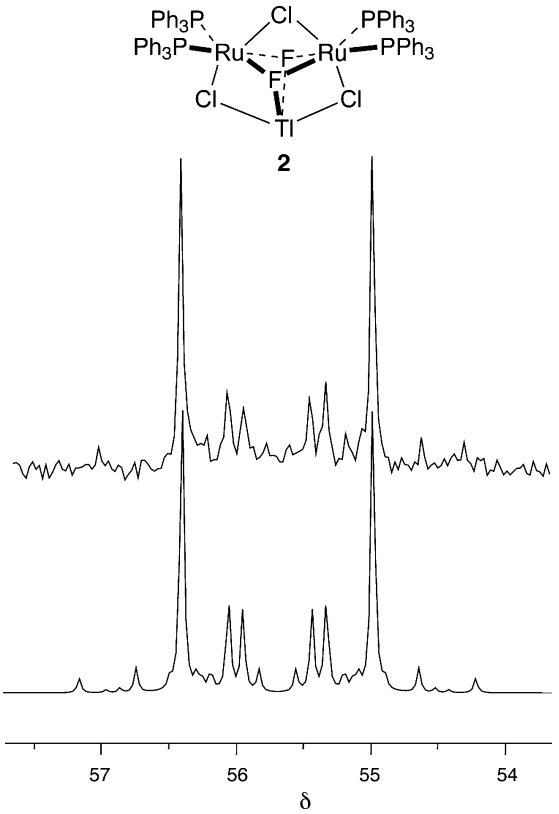

Figure 2. Experimental and simulated ^{31}P NMR spectrum of **2**.

whose ^{31}P NMR spectrum showed the signals of **2** (34%), of unreacted [RuCl$_2$(PPh$_3$)$_3$] (36%), and of other unidentified products (30%). Red crystals of **2**·CH$_2$Cl$_2$ were obtained by addition of pentane to the dichloromethane solution. On the basis of the equivalence of the bridging fluorides observed in the ^{19}F NMR spectrum (see Results and Discussion sections), the spin system was assumed as AA′(MM′)$_2$X (A = F, M = P, X = Tl) assuming a pseudo-C_{2v} symmetry for the molecule (Figure 2). As the ^{19}F NMR spectrum is broad and featureless, only the ^{31}P NMR subspectrum was simulated. ^{31}P{^{1}H} NMR (CD$_2$Cl$_2$, 121 MHz): δ 55.70 ((MM′)$_2$ part of an AA′(MM′)$_2$X spin system, $J_{P,P'} = -31.9$, $J_{P,F} = +160.8$, $J_{P,F'} = -11.5$, 4 P, $J_{F,F'} = -115.8$). ^{19}F NMR (CD$_2$Cl$_2$, 282 MHz): δ −346 (br, 2F). Anal. Calcd for C$_{72}$H$_{60}$Cl$_3$F$_2$P$_4$Ru$_2$Tl·CH$_2$Cl$_2$: C, 52.04; H, 3.71. Found: C, 52.20; H, 4.13.

[Tl(μ$_3$-F)(μ$_2$-F)(μ$_2$-X)Ru$_2$(μ$_2$-Br)(μ$_2$-F)(PPh$_3$)$_4$] (3). Complex **1** (80 mg, 69.6 μmol) and bromodiphenylmethane (18.8 mg, 76.1 mmol) were dissolved in CH$_2$Cl$_2$ (3 mL) in a Teflon vessel in a glovebox. After stirring at room temperature for 22 h, the reaction mixture was filtered through a microfilter to remove the thallium salts. CD$_2$Cl$_2$ was added to the red-brown solution, which was then analyzed by ^{1}H, ^{19}F, and ^{31}P NMR spectroscopy. The conversion of **1** was 67% (as determined by ^{31}P NMR spectroscopy). Complex [Tl(μ$_3$-F)(μ$_2$-F)(μ$_2$-X)Ru$_2$(μ$_2$-Br)(μ$_2$-F)(PPh$_3$)$_4$] (**3**) was obtained as the only metal-containing product. Fluorodiphenylmethane (Ph$_2$CHF) was detected by ^{19}F NMR spectroscopy (CH$_2$Cl$_2$/CDCl$_3$): δ −167.2 (lit. −169,[20] d, 1F, $J_{F,H} = 46.5$ Hz, lit. 48,[20] Ph$_2$C(H)−*F*). ^{1}H NMR (CDCl$_3$): δ 6.34 (s, 1H, CBr−*H*, Ph$_2$CHBr, 63%), 6.50 (d, 1H, $J_{F,H} = 47.0$ Hz, Ph$_2$C(F)−*H* (Ph$_2$CHF), 37%).

Red crystals of **3** formed upon diffusion of pentane into the CH$_2$Cl$_2$/CDCl$_3$ solution. The C_{2v}-symmetric structure [TlRu$_2$BrF$_4$(PPh$_3$)$_4$] (Figure S1) was assumed for the simulation of the ^{31}P and ^{19}F NMR spectra of **3** with an AA′BB′(MM′)$_2$X spin system. The broad ^{19}F spectrum yielded only approximate values of $J_{F,F'}$ (−150 Hz, (μ$_2$-F)-Ru−(μ$_3$-F)) and $J_{Tl,F}$ (+2100 Hz, (μ$_2$-F)-Tl) that were not refined. ^{31}P NMR (CDCl$_3$, 121 MHz): δ 59.84 ((MM′)$_2$ part, $J_{P,P'} = -37.0$, $J_{P,F}$(*trans*) = +169.6, $J_{P,F}$(*cis*-P−Ru−(μ$_3$-F)) = +4.9, $J_{P,F}$(P−Ru−(μ$_2$-F)) = −4.3, $J_{F,F'}$((μ$_3$-F)-Ru−(μ$_3$-F)) = −133.7, 4 P). ^{19}F NMR (CDCl$_3$, 282 MHz): δ −341.7 (AA′ part, $J_{F,F'}$((μ$_2$-F)-Ru−(μ$_3$-F)) = ca. −150, 2 μ$_3$-*F*), −422.6 (BB′ part, $J_{F,F'}$((μ$_2$-F)-Ru−(μ$_2$-F)) = assumed as +100, no effect on spectral appearance, 2 μ$_2$-*F*). Anal. Calcd for C$_{72}$H$_{60}$Br$_{1.39}$F$_{3.61}$P$_4$Ru$_2$Tl: C, 52.91; H, 3.70. Found: C, 52.68; H, 4.24.

Table 1. Crystal Data and Structure Refinement for **1**−**3**

	1	**2**	**3**
formula	C$_{55}$H$_{46}$Cl$_3$F$_3$P$_3$RuTl	C$_{73}$H$_{62}$Cl$_5$F$_2$P$_4$Ru$_2$Tl	C$_{73}$H$_{61}$BrCl$_3$F$_4$P$_4$Ru$_2$Tl
fw	1268.62	1684.87	1730.87
cryst size (mm^3)	0.74 × 0.60 × 0.14	0.15 × 0.05 × 0.02	0.14 × 0.13 × 0.12
cryst syst	hexagonal	monoclinic	monoclinic
space group	$P6_3$	$P2_1/c$	$P2_1/n$
a (Å)	12.7484(18)	19.725(7)	13.1385(5)
b (Å)	12.7484(18)	14.541(6)	25.1451(9)
c (Å)	17.362(4)	26.270(10)	22.4359(7)
α (deg)	90	90	90
β (deg)	90	110.084(12)	93.053(1)
γ (deg)	120	90	90
V (Å^3)	2443.6(7)	7077(5)	7401.6(5)
Z	2	4	4
ρ_{calcd} (g/cm^{-3})	1.724	1.581	1.553
abs coeff (mm^{-1})	3.914	3.018	3.358
θ range (deg)	1.84−31.06	2.12−26.41	2.24−28.31
no. reflns collcd	19984	44840	55113
no. indep reflns	4808 [R_{int} = 0.2066]	14469 [R_{int} = 0.0393]	18386 [R_{int} = 0.0833]
no. obsd reflns	4808	10769	7416
GOF on F^2	0.988	1.065	0.842
R1 indices [$I > 2\sigma(I)$]	0.0536	0.0507	0.0568
wR2 indices (all data)	0.1420	0.1728	0.1653
largest peak/hole (e Å^{-3})	5.037/−1.863	2.022/−1.347	1.281/−1.528

X-ray Studies. X-ray studies were performed at room temperature on a Siemens SMART platform with CCD detector, normal focus molybdenum-target X-ray tube (λ = 0.71073 Å), and graphite monochromator by using ω-scans. Unit cell dimensions determination and data reduction were performed by standard procedures, and an empirical absorption correction (SADABS) was applied for **1**, but not for **2** and **3**. The structures were solved with SHELXS-96 using direct methods, and refined by full-matrix least-squares on F^2 with anisotropic displacement parameters for all non-H atoms. Hydrogen atoms were introduced at calculated positions (except for disordered solvent molecules) and refined with the riding model and individual isotropic thermal parameters. Table 1 contains some crystallographic data; atomic coordinates, anisotropic displacement coefficients, and an extended list of interatomic distances and angles of **1**−**3**, as well as the results of a preliminary X-ray structure determination of a crystal from the mixed sample of **1** and **2**, are available as Supporting Information.

Yellow prisms of **1** were obtained (together with red crystals of **2**, see below) by diffusion of pentane into a CDCl$_3$ solution of **1** and **2**. Octants collected: *h*, −13 to 18, *k*, −18 to 17, *l*, −24 to 24. Max and min calculated transmission factors were 0.6103 and 0.1598. The Flack *x* parameter was −0.024(5). The crystal contains one CDCl$_3$ molecule as solvent of crystallization. Selected bond

(20) Lai, C.; Kim, Y. I.; Wang, C. M.; Mallouk, T. E. *J. Org. Chem.* **1993**, *58*, 1393.

Table 2. Selected Bond Distances (Å) and Angles (deg) for $[Tl(\mu\text{-}F)_3Ru(PPh_3)_3]$ (**1**)

Tl−F	2.389(4)	Ru−F	2.133(3)
Ru−P	2.3239(14)	Ru···Tl	3.3446(9)
F···C(2)	2.925(5)	F···C(2)	2.09
F−Tl−F′	66.73(13)	F−Ru−F′	76.03(15)
P−Ru−P′	97.79(5)	Ru−F−Tl	95.25(12)
P−Ru−F	99.80(10)	P−Ru−F′	161.50(10)
P−Ru−F″	85.47(10)		

Table 3. Selected Bond Distances (Å) and Angles (deg) for $[Tl(\mu_3\text{-}F)Ru_2Cl_2(\mu_2\text{-}Cl)(\mu_2\text{-}F)(PPh_3)_4]$ (**2**)

Tl−Cl(4)	3.0195(19)	Tl−Cl(5)	2.9719(17)
Tl−F(1)	2.668(3)	Tl···F(2)	3.101(3)
Ru(1)−F(1)	2.195(3)	Ru(2)−F(1)	2.209(3)
Ru(1)−F(2)	2.211(3)	Ru(2)−F(2)	2.242(4)
Ru(1)−Cl(3)	2.3785(16)	Ru(2)−Cl(3)	2.3709(16)
Ru(1)−Cl(4)	2.4130(16)	Ru(2)−Cl(5)	2.4038(16)
Ru(1)−P(1)	2.2677(16)	Ru(2)−P(3)	2.2848(17)
Ru(1)−P(2)	2.2766(15)	Ru(2)−P(4)	2.2686(17)
Tl···Ru(1)	3.7835(12)	Tl···Ru(2)	3.7783(11)
Ru(1)···Ru(2)	3.1909(11)	F(2)···H−C(8)	2.26
F(1)···H−C(62)	2.14	F(2)···H−C(50)	2.14
Cl(4)···H−C(20)	2.67	Cl(5)···H−C(38)	2.50
F(1)−Tl−Cl(4)	68.76(7)	F(1)−Tl−Cl(5)	69.92(7)
Cl(4)−Tl−Cl(5)	127.33(4)	Ru(1)−Cl(3)−Ru(2)	84.42(5)
Tl−F(1)−Ru(1)	101.71(12)	Tl−F(1)−Ru(2)	101.13(11)
Tl−Cl(4)−Ru(1)	87.54(5)	Tl−Cl(5)−Ru(2)	88.66(5)
Ru(1)−F(1)−Ru(2)	92.84(11)	Ru(1)−F(2)−Ru(2)	91.56(13)
F(1)−Ru(1)−F(2)	71.03(12)	F(1)−Ru(2)−F(2)	70.19(12)
F(1)−Ru(1)−Cl(3)	77.78(9)	F(1)−Ru(2)−Cl(3)	77.67(9)
F(1)−Ru(1)−Cl(4)	88.68(9)	F(2)−Ru(2)−Cl(5)	88.41(9)
F(1)−Ru(1)−P(1)	162.45(9)	F(1)−Ru(2)−P(3)	166.21(9)
F(1)−Ru(1)−P(2)	96.36(9)	F(1)−Ru(2)−P(4)	92.46(9)
F(2)−Ru(1)−Cl(3)	79.39(9)	F(2)−Ru(2)−Cl(3)	78.94(9)
F(2)−Ru(1)−Cl(4)	90.13(9)	F(1)−Ru(2)−Cl(5)	89.17(9)
F(2)−Ru(1)−P(1)	91.96(10)	F(2)−Ru(2)−P(3)	99.86(9)
F(2)−Ru(1)−P(2)	166.92(10)	F(2)−Ru(2)−P(4)	162.61(9)
Cl(3)−Ru(1)−Cl(4)	164.96(5)	Cl(3)−Ru(2)−Cl(5)	164.17(5)
Cl(3)−Ru(1)−P(1)	95.28(6)	Cl(3)−Ru(2)−P(3)	91.26(6)
Cl(3)−Ru(1)−P(2)	94.84(5)	Cl(3)−Ru(2)−P(4)	99.03(5)
Cl(4)−Ru(1)−P(1)	95.83(6)	Cl(5)−Ru(2)−P(3)	100.34(6)
Cl(4)−Ru(1)−P(2)	93.11(6)	Cl(5)−Ru(2)−P(4)	90.18(6)
P(1)−Ru(1)−P(2)	100.30(6)	P(3)−Ru(2)−P(4)	97.44(6)

lengths and angles are given in Table 2. Complex **2** was identified in a preliminary X-ray study carried out on a red crystal from the reaction of $[RuCl_2(PPh_3)_3]$ with TlF (3 equiv), which yielded the mixture of **1** and **2** mentioned above. The following X-ray analysis of a red prism (obtained by diffusion of pentane into CH_2Cl_2) obtained from the synthesis with 0.5 equiv of TlF confirmed the identity of **2**. All reported data refer to the latter crystal. Octants collected: *h*, −21 to 24, *k*, −17 to 18, *l*, −32 to 27. Max and min calculated transmission factors were 0.9477 and 0.6603. A CH_2Cl_2 molecule was detected in three different sites with occupancies refined to 0.79(1), 0.43(1), and 0.36(1). Selected bond lengths and angles are given in Table 3. Red prisms of **3** were obtained by diffusion of pentane into a $CH_2Cl_2/CDCl_3$ solution at room temperature. Octants collected: *h*, −17 to 15, *k*, −27 to 33, *l*, −29 to 19. Max and min calculated transmission factors were 0.6887 and 0.6507. The crystal contained one $CDCl_3$ molecule as solvent of crystallization. Selected bond lengths and angles are given in Table 4.

Reaction of 1 with H_2 in $CDCl_3$. Compound **1** (20 mg, 17.4 μmol) was dissolved in $CDCl_3$ (1 mL) in an NMR tube, and H_2 gas was bubbled through the solution for 5 min. Within seconds, the color turned from yellow to dark red, and small amounts of a colorless solid precipitated. The ^1H and ^{19}F NMR spectra of the reaction solution indicated the formation of $[Ru(H)Cl(PPh_3)_3]$.[21] ^1H NMR ($CDCl_3$, 25 °C): $\delta = -17.4$ (q, $J_{P,H} = 26$ Hz, 1 H, Ru−*H*), 6.9−7.4 (m, 45 H, aromatic H). $^{31}P\{^1H\}$ NMR ($CDCl_3$, 25 °C): δ 58.5 (br, 3 P). ^1H NMR ($CDCl_3$, −60 °C): δ −18.5 (dt, $J_{P(eq),H} = 34$ Hz, $J_{P(ax),H} = 22$ Hz, 1 H, Ru−*H*), 6.9−7.4 (m, 45 H, aromatic H). $^{31}P\{^1H\}$ NMR ($CDCl_3$, −60 °C): δ 39.7 (d, $J_{P,P'} = 29$ Hz, 1 P, equatorial *P*), 95.3 (t, $J_{PP} = 29$ Hz, 2 P, axial *P*).

Table 4. Selected Bond Distances (Å) and Angles (deg) for $[Tl(\mu_3\text{-}F)(\mu_2\text{-}F)(\mu_2\text{-}X)Ru_2(\mu_2\text{-}Br)(\mu_2\text{-}F)(PPh_3)_4]$ (**3**)

Tl−F(4)	2.503(4)	Tl−F/Br(5)	2.804(9)/ 2.989(3)
Tl−F(1)	2.694(4)	Tl···F(2)	2.843(4)
Ru(1)−F(1)	2.153(4)	Ru(2)−F(1)	2.161(4)
Ru(1)−F(2)	2.150(4)	Ru(2)−F(2)	2.168(4)
Ru(1)−Br(3)	2.476(12)	Ru(2)−Br(3)	2.4754(12)
Ru(1)−F(4)	2.067(4)	Ru(2)−F/Br(5)	2.247(9)/ 2.461(3)
Ru(1)−P(1)	2.244(2)	Ru(2)−P(3)	2.254(2)
Ru(1)−P(2)	2.2711(19)	Ru(2)−P(4)	2.248(2)
Tl···Ru(1)	3.5316(7)	Tl···Ru(2)	3.7217(8)
Ru(1)···Ru(2)	3.1396(9)	F(2)···H−C(8)	2.15
F(1)···H−C(30)	2.24	F(2)···H−C(50)	2.34
F(1)···H−C(62)	2.44	F/Br(5)···H−C(38)	2.28/1.88
F(4)···H−C(24)	2.16	F/Br(5)···H−C(62)	2.21/2.83
F(1)−Tl−F(4)	67.20(12)	F(1)−Tl−F/Br(5)	62.8(2)/ 71.6(1)
F(4)−Tl−F/Br(5)	123.2(2)/ 125.3(1)	Ru(1)−Br(3)−Ru(2)	78.73(4)
Tl−F(1)−Ru(1)	92.84(14)	Tl−F(1)−Ru(2)	99.49(14)
Tl−F(4)−Ru(1)	100.78(16)	Tl−F/Br(5)−Ru(2)	94.3(3)/ 85.6(1)
Ru(1)−F(1)−Ru(2)	93.39(16)	Ru(1)−F(2)−Ru(2)	93.28(15)
F(1)−Ru(1)−F(2)	70.77(16)	F(1)−Ru(2)−F(2)	70.30(15)
F(1)−Ru(1)−Br(3)	80.64(11)	F(1)−Ru(2)−Br(3)	80.47(11)
F(1)−Ru(1)−F(4)	86.07(16)	F(2)−Ru(2)−F/Br(5)	87.6(3)/ 82.3(1)
F(1)−Ru(1)−P(1)	165.67(12)	F(1)−Ru(2)−P(3)	169.24(13)
F(1)−Ru(1)−P(2)	96.78(12)	F(1)−Ru(2)−P(4)	91.75(12)
F(2)−Ru(1)−Br(3)	79.48(11)	F(2)−Ru(2)−Br(3)	79.14(12)
F(2)−Ru(1)−F(4)	84.70(15)	F(1)−Ru(2)−F/Br(5)	81.1(3)/ 92.0(1)
F(2)−Ru(1)−P(1)	94.91(13)	F(2)−Ru(2)−P(3)	99.36(13)
F(2)−Ru(1)−P(2)	167.12(13)	F(2)−Ru(2)−P(4)	161.67(12)
Br(3)−Ru(1)−F(4)	161.98(12)	Br(3)−Ru(2)−F/Br(5)	160.1(3)/ 161.43(9)
Br(3)−Ru(1)−P(1)	96.55(6)	Br(3)−Ru(2)−P(3)	94.89(9)
Br(3)−Ru(1)−P(2)	95.54(6)	Br(3)−Ru(2)−P(4)	94.69(6)
F(4)−Ru(1)−P(1)	93.32(13)	F/Br(5)−Ru(2)−P(3)	101.9(3)/ 89.4(1)
F(4)−Ru(1)−P(2)	98.08(12)	F/Br(5)−Ru(2)−P(4)	93.3(3)/ 102.6(1)
P(1)−Ru(1)−P(2)	97.48(7)	P(3)−Ru(2)−P(4)	98.34(9)

Reaction of 1 with H_2 in THF-d_8. Compound **1** (20 mg, 17.4 μmol) was dissolved in THF-d_8 (1 mL) in an NMR tube, and H_2 gas was bubbled through the solution for 10 min, during which the solution color changed from yellow to light brown. Small amounts of a colorless solid (TlF) precipitated. The ^1H and ^{31}P NMR spectra indicated the formation of $[Ru(H)_2(H_2)(PPh_3)_3]$.[22] ^1H NMR (THF-d_8, 25 °C): δ −7.57 (br s, 4 H, Ru−*H*), 6.91−7.22 (m, 45 H, aromatic H). $^{31}P\{^1H\}$ NMR (THF-d_8, 25 °C): δ 56.8 (s, 3 P). ^1H NMR (THF-d_8, −100 °C): δ −7.57 (br s, 4 H, Ru−*H*),

(21) (a) Hallman, P. S.; Evans, D.; Osborn, J. A.; Wilkinson, G. *J. Chem. Soc., Chem. Commun.* **1967**, 305. (b) Hallman, P. S.; McGarvey, B. R.; Wilkinson, G. *J. Chem. Soc. A* **1968**, 3143.

(22) (a) Harris, R. O.; Hota, N. K.; Sadavoy, L.; Yuen, J. M. C. *J. Organomet. Chem.* **1973**, *54*, 259. (b) Ashworth, T. V.; Singleton, E. *J. Chem. Soc., Chem. Commun.* **1976**, 706. (c) Hamilton, D. G.; Crabtree, R. H. *J. Am. Chem. Soc.* **1988**, *110*, 4126. (d) Van Der Sluys, L. S.; Kubas, G. J.; Caulton, K. G. *Organometallics* **1991**, *10*, 1033.

Table 5. Hardness Parameters of F• and FHF from Calculated *I* and *A*

species	*E*(total) (hartree)	*A*[a] (eV)	*I*[a] (eV)	η[b] (eV)	model[c]	*d*	F···F (Å)
F^-	−99.418586	1.28			HF	spe	
	−99.623847	3.40			MP2	spe	
	−99.620258	3.02			CCSD	spe	
		(3.40)					
F•	−99.371652			7.24	HF	spe	
	−99.498820			6.84	MP2	spe	
	−99.509397			7.00	CCSD	spe	
				(7.01)			
F^+[e]	−98.792661		15.76		HF	spe	
	−98.871069		17.08		MP2	spe	
	−98.884217		17.01		CCSD	spe	
			(17.42)				
FHF^-[f]	−199.488606	3.15			HF	eqg	2.268
	−199.885603	6.16			MP2	eqg	2.329
	−199.883831	4.93			CCSD	spe	2.329
FHF[f]	−199.372931			5.20	HF	eqg	3.121[g]
	−199.659182			4.04	MP2	eqg	2.980[h]
	−199.702798			5.00	CCSD	spe	2.980[h]
FHF^+[e,f]	−198.874702		13.56		HF	eqg	2.383
	−199.135370		14.25		MP2	eqg	2.429
	−199.154050		14.93		CCSD	spe	2.429

[a] Experimental values (from ref 44) in parentheses. [b] Defined as $\eta = (I - A)/2$. [c] HF = HF/6-31+G*//HF/6-31+G*, MP2 = MP2/6-31+G*//MP2/6-31+G*, CC = CCSD/6-31+G*//MP2/6-31+G*. [d] Single point energy (spe) or equilibrium geometry (eqg). [e] $S = 1$. [f] Corrected for thermal energy ($T = 298.15$ K, $P = 1$ atm). [g] H−F distances are 0.914 and 2.207 Å. [h] H−F distances are 0.934 and 2.046 Å.

6.91−7.22 (m, 45 H, aromatic H). $^{31}P\{^1H\}$ NMR (THF-d_8, 25 °C): δ 60.1 (br d, $J_{PP} = \sim 20$ Hz, 2 P), 48.8 (br t, $J_{PP} = \sim 20$ Hz, 1 P).

Calculations. Calculations were performed by using Spartan'02 (Wavefunction, Inc., Irvine, CA). Single point energies of F•, F^-, and F^+ were determined at the HF, MP2, and CCSD levels with the 6-31+G* basis set. The geometries of FHF^-, FHF•, and FHF^+ were optimized at the HF/6-31+G* and MP2/6-31+G* level. Additionally, single point energies were calculated at the CCSD level by using the corresponding MP2 optimized geometries. Distances and energies (corrected for thermal energy, 298.15 K) are given in Table 5. All species are linear. The FHF^- anion and the FHF^+ cation are centrosymmetric ($D_{\infty h}$), whereas FHF• has $C_{\infty v}$ symmetry and can be described as F′−H···F•. Frequency calculations (zero imaginary) indicated that all structures correspond to energy minima. The MP2/6-31+G* frequencies of FHF^- are in reasonable agreement with experimental values: 604 (sym stretching, expt 600−615), 1231 cm^{-1} (asym stretching, expt 1284−1563), and 1288 (2-fold degenerate bending, expt 1199−1274).[23] In F′−H···F•, the spin density is concentrated on F• (1.00), and it is 0.00 on H and F′. The Mulliken charges are −0.51 (F′), +0.49 (H), and +0.02 (F•). In the FHF^+ biradical, the Mulliken charges are F (+0.14), H (+0.72).

Results

Reaction of [RuCl$_2$(PPh$_3$)$_3$] with TlF. Preliminary attempts of halide metathesis between [RuCl$_2$(PPh$_3$)$_3$] and silver or cesium fluoride in dichloromethane solution were unsuccessful. The reaction with AgF in CH_2Cl_2 led to extensive decomposition to unidentified products, probably owing to the traces of moisture invariably present in the salt. Although CsF can be dried easily, its reaction with [RuCl$_2$(PPh$_3$)$_3$] in CH_2Cl_2 led to a mixture of several products (presumably polynuclear complexes), which could neither be isolated nor identified.

Scheme 1. Synthesis of [Tl(μ-F)$_3$Ru(PPh$_3$)$_3$] (**1**) and [RuCl$_3$F$_2$(PPh$_3$)$_4$Tl] (**2**)

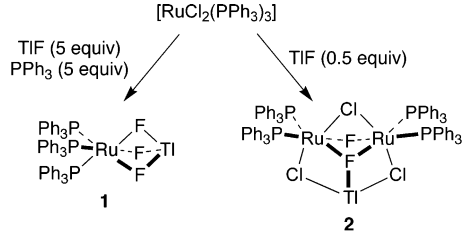

As thallium(I) fluoride is available as anhydrous salt and forms insoluble chlorides, it is an ideal candidate for chloride−fluoride metathesis. The reaction of [RuCl$_2$(PPh$_3$)$_3$] with TlF (3 equiv) in dichloromethane at room temperature yielded a mixture of products and uncoordinated PPh_3, as indicated by the ^{31}P NMR spectrum of the reaction solution. The two major products were identified as [Tl(μ-F)$_3$Ru(PPh$_3$)$_3$] (**1**) and [Tl(μ$_3$-F)(μ$_2$-Cl)$_2$Ru$_2$(μ$_2$-Cl)(μ$_2$-F)(PPh$_3$)$_4$] (**2**) (see below). Pure **1** was obtained by adding an excess of PPh_3 (5 equiv) to the reaction solution (Scheme 1), which suppresses PPh_3 dissociation and the formation of **2**.

The formulation of [Tl(μ-F)$_3$Ru(PPh$_3$)$_3$] (**1**) is supported by ^{31}P and ^{19}F NMR spectroscopy, elemental analysis, and an X-ray study. As already observed for other fluoro complexes,[5] traces of water in the solvents ($CDCl_3$ or CD_2Cl_2) lead to the loss of P,F-coupling in the ^{31}P NMR subspectrum and to the disappearance of the ^{19}F NMR signal of **1**. Furthermore, the ^{31}P and ^{19}F NMR spectra of **1** in CD_2Cl_2 or $CDCl_3$ are temperature-dependent, which hints to the occurrence of a yet unidentified dynamic process. As **1** is a nonelectrolyte in CH_2Cl_2, this process probably does not involve ionization. Resolved NMR spectra were obtained at −20 °C (^{31}P) and at −60 °C (^{19}F) in CD_2Cl_2 dried over molecular sieves. The ^{31}P NMR spectrum of [Tl(μ-F)$_3$Ru(PPh$_3$)$_3$] (**1**) at −20 °C was simulated as the MM′M″ part of the total AA′A″MM′M″X spin system (Figure 1 and Experimental Section). The room temperature ^{19}F NMR spectrum of [Tl(μ-F)$_3$Ru(PPh$_3$)$_3$] (AA′A″ part) shows a broad doublet with a splitting of about 1060 Hz. The resolved spectrum obtained at −60 °C is a doublet of doublets whose simulation gave $^1J_{Tl,F} = 890$ Hz besides the same *trans*-$J_{P,F}$ coupling constant (201 Hz) found for the ^{31}P (MM′M″) subspectrum.

Complex **2** was obtained as the main product (34% yield) by reacting [RuCl$_2$(PPh$_3$)$_3$] with TlF (0.5 equiv) in CH_2Cl_2. Unreacted [RuCl$_2$(PPh$_3$)$_3$] (36%) and other unidentified products (30%) were detected by ^{31}P NMR spectroscopy. Crystallization from CH_2Cl_2/pentane yielded pure **2**, which was studied by X-ray crystallography (see below). The ^{19}F NMR spectrum is a broad and featureless signal at δ −346 with a line width $w_{1/2}$ of 360 Hz, which is much less than the expected splitting caused by Tl−F coupling. In fact, the $^1J_{Tl,F}$ coupling constant is expected to be not less than 800 Hz on the basis of the NMR spectra of **1** and of [Tl(μ-F)$_2$Ru(dppe)$_2$]$^+$.[14] As this suggests that fast chemical exchange between the Tl-bound and the Tl-unbound fluorides occurs,

(23) Panich, A. M. *Chem. Phys.* **1995**, *196*, 511.

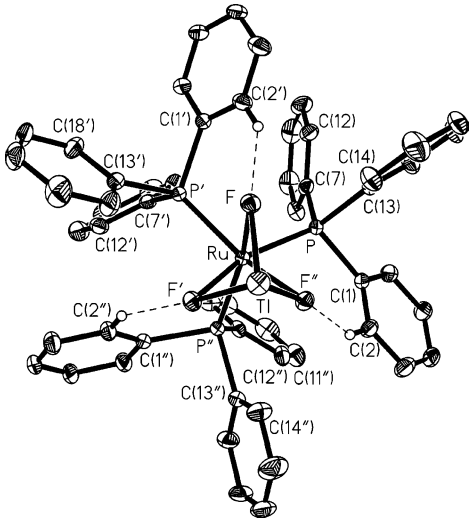

Figure 3. ORTEP view of $[Tl(\mu\text{-}F)_3Ru(PPh_3)_3]$ (**1**) (30% probability ellipsoids).

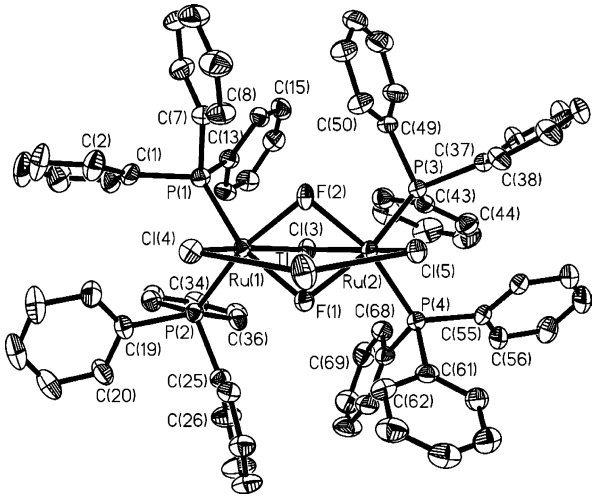

Figure 4. ORTEP view of $[Tl(\mu_3\text{-}F)(\mu_2\text{-}Cl)_2Ru_2(\mu_2\text{-}Cl)(\mu_2\text{-}F)(PPh_3)_4]$ (**2**) (30% probability ellipsoids).

pseudo-C_{2v} symmetry was assumed for complex **2** in solution. Thus, the ^{31}P NMR subspectrum was simulated as the $(MM')_2$ part of an $AA'(MM')_2X$ spin system (see Figure 2 and Experimental Section).

X-ray Structure of $[Tl(\mu\text{-}F)_3Ru(PPh_3)_3]$ (1). Yellow crystals of **1** belonging to the hexagonal $P6_3$ space group were grown from $CDCl_3$/pentane. The Tl and Ru atoms lie on a crystallographic 6_3 axis. The F, P, and C atoms in general positions generate the rest of the molecule (Figure 3). The complex can be described as being composed by a pseudo-octahedral $[RuF_3(PPh_3)_3]^-$ anion and a Tl^+ cation capping the F_3 face. The Tl−F−Ru bridge is slightly stretched at the fluoride pivots (the Tl−F−Ru angle is 95.2(1) °), which allows for a nonbonded Ru···Tl distance of 3.3446(9) Å. This is slightly shorter than in the doubly F-bridged $[Tl(\mu\text{-}F)_2Ru(dppe)_2)]^+$, in which the Ru···Tl distance is 3.6640(8) Å.[14]

The triple (μ-F) bridge causes a distortion of the pseudo-octahedral geometry at ruthenium. The *trans*-P−Ru−F angle is 161.5(1)°, and the F−Ru−F′ angles are closed down to 76.03(15)° (Table 2). Thus, the F−Ru−F angle in **1** is smaller than in $[Tl(\mu\text{-}F)_2Ru(dppe)_2]^+$ (77.9(3)°)[14] and in *cis*-$[RuF_2(dppp)_2]$) (78.2(1)°).[13b] The small F−Ru−F′ angles in **1** release the steric strain around ruthenium and allow for relatively large P−Ru−F and P−Ru−P′ angles of 99.8(1)° and 97.79(5)°, respectively. Analogous effects have been observed in $[Tl(\mu\text{-}F)_2Ru(dppe)_2]^+$ and *cis*-$[RuF_2(dppp)_2]$.[14,13b] The Ru−F bond length in **1** (2.133(3) Å) is comparable to those of the closely related $[Tl(\mu\text{-}F_2)Ru(dppe)_2]^+$ (2.112(7) and 2.119(7) Å).[14] Both values are significantly longer than in the related terminal fluoro complexes *cis*-$[RuF_2(dppp)_2]$ (2.069(3) and 2.056(3) Å)[13b] and *cis*,*cis*,*trans*-$[RuF_2(CO)_2(PPh_3)_2]$ (2.011(4) Å).[9a] The most interesting comparison is between **1** and the recently reported confacial bioctahedral cation $[Ru_2(\mu\text{-}F)_3(PEt_3)_6]^+$,[16] which features similar Ru−F distances (in the range 2.132(2)−2.170(2) Å vs 2.133(3) Å in **1**) and an average F−Ru−F angle of 73.7° (vs 76.0(2)° in **1**).

The Ru−P distance (2.324(1) Å) is unexceptional. A H···F nonbonded contact between the fluoro ligand and the *ortho* H atom on C(2) of a phenyl ring is significantly shorter than the sum of the van der Waals radii of F and H (ca. 2.7 Å). On the basis of the Ru···C(2) distance of 2.925(5) Å, a H···F distance of 2.09 Å is calculated by assuming d(C−H) = 0.93 Å. Similar contacts have been considered as weak C−H···F hydrogen bonds.[13b,24]

Literature data about Tl−F bond lengths are very rare. The Tl−F distance in **1** (2.389(4) Å) is shorter than in $[Tl(\mu\text{-}F)_2Ru(dppe)_2]$ (2.419(7) and 2.419(8) Å) and in a Tl(III) fluoro porphyrin (2.441(6) Å),[25] which can be ascribed to the effect of the triple bridge. These Tl−F distances are considerably shorter than in the (μ_3-F)-Tl units of fluoro aluminates (in the range 2.528(6)−2.598(7) Å)[26] or in C−F···Tl linkages between thallium(I) and nonionic fluorine (2.952(5)−3.048(5) Å).[27] The closest nonbonded contact of the Tl atom in **1** is to a C atom of a neighboring molecule (Tl···C(11) = 3.958(3) Å). The closest intramolecular contact is Tl···C(14) (4.174(4) Å).

X-ray Structure of $[Tl(\mu_3\text{-}F)(\mu_2\text{-}Cl)_2Ru_2(\mu_2\text{-}Cl)(\mu_2\text{-}F)(PPh_3)_4]$ (2). Complex **2** crystallized as red prisms from dichloromethane/pentane. The core of the trimetallic complex is a confacial $Ru_2F_2Cl_3P_4$ bioctahedron (Figures 4 and 5). The Tl atom lies on the shared face of the octahedra and binds to one of the Ru,Ru-bridging F atoms and to two Cl atoms. The F(1) atom is μ_3-bridging between Ru(1), Ru(2), and Tl. The Tl−F(2) distance is much longer than the Tl−(F(1) one (3.101(3) vs 2.668(3) Å) and is best considered as nonbonding (Table 3). Owing to the μ_3-bridging mode of

(24) (a) Coleman, K. S.; Fawcett, J.; Holloway, J. H.; Hope, E. G.; Russell, D. R. *J. Chem. Soc., Dalton Trans.* **1997**, 3557. (b) Cockman, R. W.; Ebsworth, E. A. V.; Holloway, J. H.; Murdoch, H.; Robertson, N.; Watson, P. G. In *Inorganic Fluorine Chemistry*; Thrasher, J. S., Strauss, S. H., Eds.; ACS Symposium Series 555; Americal Chemical Society: Washington, DC, 1994.
(25) Coutsolelos, A. G.; Orfanopoulos, M.; Ward, D. L. *Polyhedron* **1991**, *10*, 885.
(26) Gonsior, M.; Krossing, I.; Mitzel, N. *Z. Anorg. Allg. Chem.* **2002**, *628*, 1821.
(27) Takemura, H.; Nakashima, S.; Kon, N.; Yasutake, M.; Shinmyozu, T.; Inazu, T. *J. Am. Chem. Soc.* **2001**, *123*, 9293.

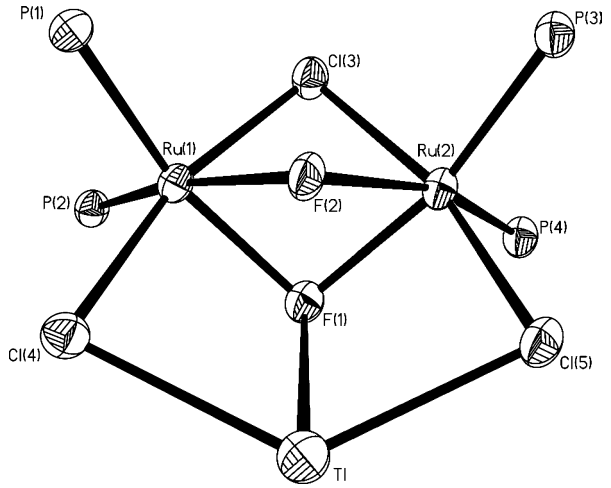

Figure 5. ORTEP view of the coordination core of [Tl(μ_3-F)(μ_2-Cl)$_2$Ru$_2$(μ_2-Cl)(μ_2-F)(PPh$_3$)$_4$] (**2**) (30% probability ellipsoids).

fluoride, the Tl−F(1) bond in **2** is longer than in **1** (2.668(3) vs 2.389(4) Å). Similar (μ_3-F)−Tl distances have been found in Tl(I)-bound fluoro aluminates (2.528(6)−2.598(7) Å).[26] The Tl−Cl distances (3.0195(19) and 2.9719(17) Å) in **2** can be compared to those of [Tl(μ-Cl)RuH(P(CH$_2$CH$_2$PPh$_2$)$_3$)] (2.815(4) Å)[28] and [TlCl$_2$Ru(PPh$_3$)(S$_3$)]$^{2+}$ (average Tl−Cl distance is 3.03 Å; S$_3$ = 1,4,7-trithiacyclononane).[29]

The octahedral coordination around Ru(1) and Ru(2) in **2** is similar to that of **1** and results in a Ru(1)···Ru(2) nonbonded distance of 3.1909(11) Å (Table 3). This is in line with the values found for confacial bioctahedral complexes of ruthenium(II), in which there are no bonding interactions between the two d^6 metals.[30] The Ru−F bond lengths in **2** are in the range 2.195(3)−2.242(4) Å (average 2.21 Å), and hence are longer than in **1** (2.133(3) Å). In particular, the Ru−F bonds to F(2) are longer than those to F(1), which is probably an effect of the different bridging modes (μ_2 vs μ_3). The Ru−F distances to the μ_2-bridging F(2) (2.211(3) and 2.242(4) Å) are longer than in [Ru$_2$(μ-F)$_3$(PEt$_3$)$_6$]$^+$ (2.15 Å)[16] and in [Ru$_2$H$_2$(μ-F)$_2$(P*i*Pr$_3$)$_4$] (2.12 Å)[31] probably owing to the effect of the bridging chloride. Although (μ-X)$_3$ bridges are common in ruthenium chemistry,[32−36] a Ru$_2$(μ_2-X)$_2$(μ_3-X)M structural motif (X = halo ligand, M = metal ion) analogous to that of **2** has only been found as part of the Ru$_3$(μ_2-Cl)$_3$(μ_3-Cl)$_2$ core.[37]

Scheme 2. Reactivity of [Tl(μ-F)$_3$Ru(PPh$_3$)$_3$] (**1**) with Dihydrogen

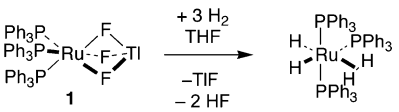

There are some short F···H−C nonbonded contacts to H atoms of the phenyl rings, but also Cl···H−C interactions (2.50, 2.67 Å) that are considerably shorter than the sum of the van der Waals radii of Cl and H, which exceeds 2.9 Å. Selected X···C distances (X = F or Cl) are given in Table 3. We have reported short intramolecular F···H−C contacts to the diphosphine ligand in [RuF(dppp)$_2$]$^+$ and *cis*-[RuF$_2$(dppp)$_2$],[13b] but also X···H−C interactions, that can be possibly described as weak hydrogen bonds, in the [RuX(dppp)$_2$]$^+$ series (X = Cl, Br, or I).[38] In a recent report, Grushin has suggested that the fluoro ligands in [(PR$_3$)(Ph)Pd(μ-F)$_2$Pd(Ph)(PR$_3$)] (R = *i*Pr or *c*-C$_6$H$_{11}$) retain a considerable basicity (as indicated by the short F···H−C contacts with the P*i*Pr$_3$ ligand or a CH$_2$Cl$_2$ molecule) despite their bridging coordination mode.[39]

Reactivity of 1. Complex **1** readily decomposes in wet CDCl$_3$ to give a mixture of products, as shown by the ^{31}P NMR spectrum of the reaction solution. The ^{19}F NMR spectrum indicates that free F$^-$ and FHF$^-$ are formed by protonolysis of the Ru−F bond. Similarly, the d^6 fluoro complex [IrF(Ph)(C$_5$Me$_5$)(PMe$_3$)] is hygroscopic and dissociates F$^-$ in wet solvents.[40] However, **1** is stable in the presence of moisture in the solid state and is therefore less reactive than *cis*-[RuF$_2$(dppp)$_2$], which readily decomposes in moist air even in the solid state and must be handled under an inert atmosphere.[13b]

The Ru−F bond of **1** undergoes hydrogenolysis readily. When [Tl(μ-F)$_3$Ru(PPh$_3$)$_3$] (**1**) was dissolved under nitrogen in THF-d_8 in an NMR tube and dihydrogen was bubbled through the reaction mixture, the yellow color of the solution turned to pale brown within minutes, and a white solid (thallium fluoride) precipitated. The ^{31}P and ^{1}H NMR spectra of the reaction solution (a singlet at δ 56.8 and a broad signal at δ −7.57, respectively) indicated that **1** was quantitatively converted into the ruthenium hydride [Ru(H)$_2$(H$_2$)(PPh$_3$)$_3$] as the only metal-containing product (Scheme 2).[22] When CD$_2$Cl$_2$ or CDCl$_3$ was used as solvent, [Ru(H)Cl(PPh$_3$)$_3$][21] was eventually formed by reaction of [Ru(H)$_2$(H$_2$)(PPh$_3$)$_3$] with the chlorinated solvent.[41]

The reactivity of **1** toward H$_2$ parallels that of [RuCl$_2$(PPh$_3$)$_3$], which is known to activate H$_2$ heterolytically in the presence of NEt$_3$ to give [RuH(Cl)(PPh$_3$)] or [RuH$_2$(H$_2$)-

(28) Bianchini, C.; Masi, D.; Linn, K.; Mealli, C.; Peruzzini, M.; Zanobini, F. *Inorg. Chem.* **1992**, *31*, 4036.
(29) Blake, A. J.; Christie, R. M.; Roberts, Y. V.; Sullivan, M. J.; Schröder, M.; Yellowlees, L. J. *J. Chem. Soc., Chem. Commun.* **1992**, 848.
(30) Knottenbelt, S. Z.; McGrady, J. E.; Heath, G. A. *J. Chem. Soc., Dalton Trans.* **2003**, 227.
(31) Coalter, J. N.; Huffman, J. C.; Streib, W. E.; Caulton, K. G. *Inorg. Chem.* **2000**, *39*, 3757.
(32) Clucas, W. A.; Armstrong, R. S.; Buys, I. E.; Hambley, T. W.; Nugent, K. W. *Inorg. Chem.* **1996**, *35*, 6789.
(33) (a) La Placa, S. J.; Ibers, J. A. *Inorg. Chem.* **1965**, *4*, 778. (b) MacFarlane, K. S.; Joshi, A. M.; Rettig, S. J.; James, B. R. *Inorg. Chem.* **1996**, *35*, 7304.
(34) (a) Raspin, K. A. *J. Chem. Soc. A* **1969**, 461. (b) Statler, J. A.; Wilkinson, G.; Thornton-Pett, M.; Hursthouse, M. B. *J. Chem. Soc., Dalton Trans.* **1984**, 1731.
(35) Rhodes, L. F.; Sorato, C.; Venanzi, L. M.; Bachechi, F. *Inorg. Chem.* **1988**, *27*, 604.
(36) Holmes, N. J.; Levason, W. L.; Webster, M. *J. Chem. Soc., Dalton Trans.* **1997**, 4223.
(37) (a) Mashima, K.; Hino, T.; Takaya, H. *Tetrahedron Lett.* **1991**, *32*, 3101. (b) Mashima, K.; Hino, T.; Takaya, H. *J. Chem. Soc., Dalton Trans.* **1992**, 2099. (c) Mashima, K.; Komura, N.; Yamagata, T.; Tani, K.; Haga, M. *Inorg. Chem.* **1997**, *36*, 2908. (d) Liu, S. H.; Yang, S. Y.; Lo, S. T.; Xu, Z. T.; Ng, W. S.; Wen, T. B.; Zhou, Z. Y.; Lin, Z. Y.; Lau, C. P., Jia, G. C. *Organometallics* **2001**, *20*, 4161.
(38) Barthazy, P.; Broggini, D.; Mezzetti, A. *Can. J. Chem.* **2001**, *79*, 904.
(39) Grushin, V. V.; Marshall, W. J. *Angew. Chem., Int. Ed.* **2002**, *41*, 4476.
(40) Veltheer, J. E.; Burger, P.; Bergman, R. G. *J. Am. Chem. Soc.* **1995**, *117*, 12478.
(41) For a related reaction, see: Christ, M. L.; Sabo-Etienne, S.; Chaudret, B. *Organometallics* **1994**, *13*, 3800.

Scheme 3. Reactivity of $[Tl(\mu\text{-}F)_3Ru(PPh_3)_3]$ (**1**) with Ph_2CHBr

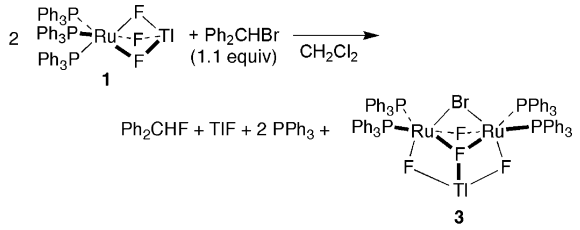

$(PPh_3)_3$] when a stronger base (such as NaOH) is used.[42] In an initial step, dihydrogen probably induces the dissociation of thallium fluoride from **1** to form an elusive $[RuF_2(PPh_3)_3]$ intermediate analogous to $[RuCl_2(PPh_3)_3]$, which can add dihydrogen to form an acidic (η^2-H_2) complex[43] that undergoes hydrogenolysis. However, neither of these species was detected by NMR spectroscopy. In fact, contrary to what is observed with $[RuCl_2(PPh_3)_3]$, the hydrogenolysis of the Ru−F bond occurs without the presence of a base. This reaction is a common feature of fluoro complexes of ruthenium,[10,13] as it is driven by the thermodynamically favored formation of HF.

As a formal adduct of $[RuF_2(PPh_3)_3]$ with TlF, $[Tl(\mu\text{-}F)_3Ru(PPh_3)_3]$ (**1**) is a shuttle of thallium(I) fluoride in solvents of low polarity. Therefore, we investigated the reaction of **1** with alkyl bromides (*tert*-butyl bromide, 1-bromo-1-phenylethane, and bromodiphenylmethane) with the dual goal of preparing $[RuF_2(PPh_3)_3]$ and developing a new reagent for the nucleophilic fluorination of alkyl bromides.[13,14] Complex **1** and the alkyl bromide were dissolved in CH_2Cl_2 under argon, and the reaction solution was sampled and analyzed by ^{31}P and ^{19}F NMR spectroscopy. Bromodiphenylmethane (1.1 equiv vs **1**) reacted with **1** to form Ph_2CHF as the only product (33% yield), as indicated by the ^1H and ^{19}F NMR spectra of the reaction solution (Scheme 3). After 22 h of reaction time, the ^{31}P NMR spectrum showed the presence of the mixed-halide trimetallic complex $[Tl(\mu_3\text{-}F)(\mu_2\text{-}F)(\mu_2\text{-}X)Ru_2(\mu_2\text{-}Br)(\mu_2\text{-}F)(PPh_3)_4]$ (X = F or Br) (**3**) (67% yield) along with unreacted **1** (33% of starting). The yields observed for the above reaction suggest the stoichiometry shown in Scheme 3,[44] in which Ph_2CHBr reacts with two equiv of **1** to give **3** (1 equiv) and Ph_2CHF (1 equiv). Thallium(I) fluoride precipitates from the solution and is thus lost in a nonproductive fashion. Complex **3** crystallized upon diffusion of pentane into the $CH_2Cl_2/CDCl_3$ reaction solution and was characterized by X-ray (see below).

Less activated substrates led to sluggish reactions with **1** and to the formation of mixtures of products that could not be analyzed. Thus, **1** reacted with *tert*-butyl bromide (5 equiv) to produce some $(CH_3)_3CF$ (detected by ^{19}F NMR spectroscopy), but the conversion of **1** was only ca. 34% after 3 days of reaction time. The ^{31}P NMR spectrum of the reaction indicated that a mixture of several unidentified complexes having ^{31}P and ^{19}F spectral patterns similar to those of **2** was formed (see below). Using a large excess of *tert*-butyl bromide (100 equiv vs **1**) did not significantly improve the total conversion of **1** (37%). In this case, **3** was formed as the major product (more than 90% selectivity). Complex **1** reacted quantitatively with a large excess (200 equiv) of 1-bromo-1-phenylethane within 22 h to give several metal complexes that were not identified.

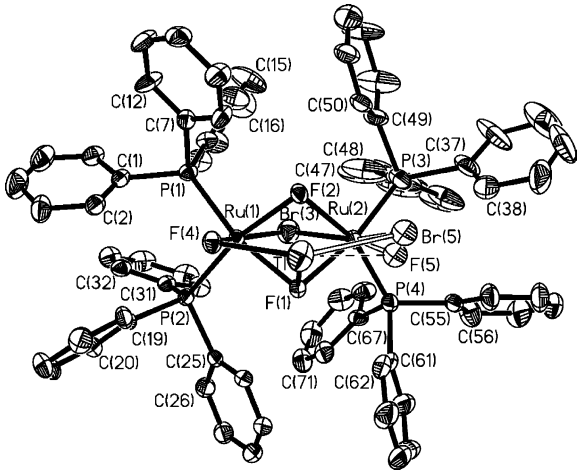

Figure 6. ORTEP view of $[Tl(\mu_3\text{-}F)(\mu_2\text{-}X)_2Ru_2(\mu_2\text{-}Br)(\mu_2\text{-}F)(PPh_3)_4]$ (**3**) (30% probability ellipsoids).

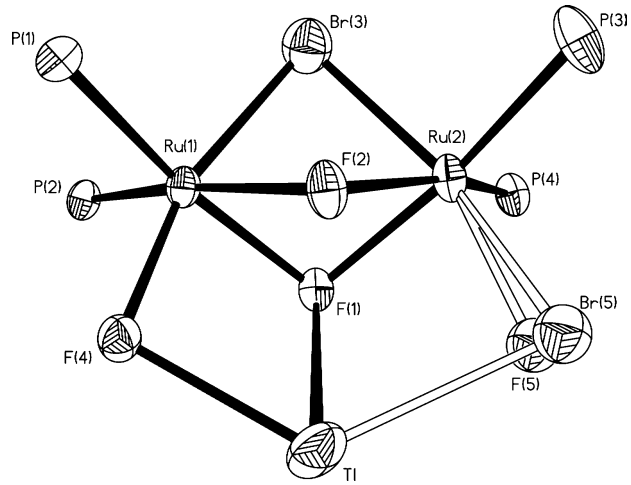

Figure 7. ORTEP view of the coordination core of $[Tl(\mu_3\text{-}F)(\mu_2\text{-}X)_2Ru_2(\mu_2\text{-}Br)(\mu_2\text{-}F)(PPh_3)_4]$ (**3**) (30% probability ellipsoids).

X-ray Structure and ^{31}P and ^{19}F NMR Spectra of 3. Crystals of the trimetallic complex $[Tl(\mu_3\text{-}F)(\mu_2\text{-}F)(\mu_2\text{-}X)\text{-}Ru_2(\mu_2\text{-}Br)(\mu_2\text{-}F)(PPh_3)_4]$ (**3**) (X = F or Br) were obtained as red prisms from a $CH_2Cl_2/CDCl_3$/pentane solution. The overall structure (Figure 6) is similar to that of **2** (Figure 4). The coordination core of **3** (Figure 7) is analogous to that of complex **2** (Figure 5). The terminal halide ligand X(5) on Ru(2) exhibits F/Br disorder. The refinement of X with F and Br gave occupancies of 61% and 39%, respectively, and reasonable Ru−X distances (Table 4). The triple bridge linking the Ru atoms is formed by two μ_2-bridging halides, Br(3) and F(2), and by F(1), which acts as a μ_3-ligand between Tl, Ru(1), and Ru(2). The Ru−F bond lengths of the Ru(μ_2-F)Ru bridge are slightly shorter in **3** (2.150(4)−

(42) Grushin, V. V.; Vymenits, A. B.; Vol'pin, M. E. *J. Organomet. Chem.* **1990**, *382*, 185.

(43) For a discussion of the effect of F on the acidity of coordinated dihydrogen in $[RuX(\eta^2\text{-}H_2)(\text{diphosphine})_2]$, see: Xu, Z. T.; Bytheway, I.; Jia, G. C.; Lin, Z. Y. *Organometallics* **1999**, *18*, 1761.

(44) This stoichiometry is approximate, however, as **3** is, at least in the crystal analyzed by X-ray, a Br/F-mixed species with the compostition $C_{72}H_{60}Br_{1.39}F_{3.61}P_4Ru_2Tl$.

2.168(4) Å) than in **2** (2.164(4)−2.194(4) Å). Interestingly, the Ru(1)−F(4) distance of 2.067(4) Å in one Ru(μ_2-F)Tl bridge is closer to those found for the terminal Ru−F bonds, such as in *cis*-[RuF$_2$(dppp)$_2$] (2.069(3) and 2.056(3) Å),[13b] than to the Ru−F bond length in **1** (2.133(3) Å). This suggests that the (μ_2-F)−Tl interaction is weaker in **3** than in **1**. The Ru(2)−X(5), Tl−X(5), and Tl−F(4) distances are not significant owing to the F/Br disorder.

The Tl−F(1) and Tl···F(2) distances are 2.694(4) and 2.843(4) Å vs 2.635(4) and 2.973(5) Å in **2**. Although the Ru(1)−Br(3) and Ru(2)−Br(3) distances are obviously longer than the Ru(1)−Cl(3) and Ru(2)−Cl(3) ones by about 0.11 Å, the confacial RuX$_3$Ru bioctahedron is slightly less stretched in **3** than in **2**, as indicated by the Ru(1)···Ru(2) nonbonded distances of 3.1396(9) and 3.1503(9) Å, respectively. The latter feature suggests that the interaction between Tl and the terminal halide X effectively "holds together" the Ru···Ru core. Accordingly, the μ-Br-bridge is distal to thallium, which minimizes the Tl−F(4) and Tl-X(5) distances.

Like in **1** and **2**, the halide ligands form a network of hydrogen bonds to some H atoms of the phenyl rings. The shortest F···H−C contacts are F(2)···H−C(8) (2.15 Å) and F(4)···H−C(24) (2.16 Å), whereas the short Br(5)···H−C(38) distance is physically meaningless and clearly an artifact of disorder.

The similarity of **2** and **3** and the F/Br disorder observed in **3** indicate that the trinuclear framework of **2** and **3** maintains its stability within a range of different halide combinations. The comparison between **1**, **2**, and **3** indicates that the Ru(μ_2-X)Ru linkage (X = F, Cl, or Br) is stable provided that one halide X is chloride or bromide. The failure to observe complexes containing a Ru(μ_2-F)Ru core among the products of **1** hints to the possibility that the bulky PPh$_3$ ligands would cause severe steric crowding in the hypothetical binuclear complex [Ru$_2$(μ-F)$_3$(PPh$_3$)$_6$]$^+$. In the reaction of [RuCl$_2$(PPh$_3$)$_3$] with TlF, the first halide exchange probably produces the hypothetical intermediate [RuClF(PPh$_3$)$_3$], which aggregates to **2** by dissociation of PPh$_3$ and addition of the Tl(I)Cl formed in the reaction. The tendency of the mixed-halide species to aggregation explains why the stoichiometric reaction of **1** with alkyl bromides is not quantitative: after the first halide metathesis between **1** and R−Br, the resulting mixed-halide species aggregates to **3**.

The room-temperature ^{19}F NMR spectrum of **3** shows signals at δ = −341.7 and −422.6. The latter, a doublet of poorly resolved multiplets with an exceptionally large $J_{Tl,F}$ coupling constant (2100 Hz), is attributed to the fluorides of the Ru−F−Tl bridges. The signal of the fluoro ligands in the Ru−F−Ru bridge (δ −341.7, $w_{1/2}$ = 375 Hz) is a broad, tripletlike signal owing to the coupling with the two F atoms of the Ru−(μ_2-F)−Tl bridges ($J_{F,F'}$ ca. 150 Hz) (Figure S1, Supporting Information). The $w_{1/2}$ of 375 Hz is smaller than the expected Tl−F coupling constant (which should be around 800 Hz), which is attributed to the fast flipping of the Tl(I) ion between the fluoro ligands of the two nonequivalent Ru−F−Tl bridges as already assumed for **2**. As the dynamic process is fast on the NMR time scale even at −60 °C, the simulation of the ^{19}F NMR spectrum yielded a qualitative agreement with the experimental one but no exact spectral parameters. The ^{31}P NMR spectrum of **3** (Figure S2, Supporting Information) is analogous to that of **2** (Figure 2) and was simulated as the (MM′)$_2$ part of an AA′BB′(MM′)$_2$X spin system by assuming the C_{2v}-symmetric structure [Tl(μ_3-F)$_2$(μ_2-F)$_2$Ru$_2$(μ_2-Br)P$_4$] (see Experimental Section). Finally, on the basis of the similarity of their spectra, we assign the ^{31}P NMR signals of the unidentified byproducts of the reactions of **1** with R−Br to structural analogues of **3** containing a different halide set.

Attempted Catalytic Fluorination. Along the lines previously developed for [RuF(P−P)$_2$]$^+$ (P−P = dppp or dppe),[13,14] we tried to turn the stoichiometric fluorination of alkyl bromides by **1** into a catalytic reaction. However, 1-bromo-1-phenylethane did not react with thallium(I) fluoride (1.1 equiv) in the presence of **1** (10 mol %) as catalyst in CH_2Cl_2 solution. No fluorinated product was observed even after 48 h. This suggests that the dissociation of TlF from **1** is required for catalytic activity. With an excess of thallium fluoride present in the reaction mixture, the equilibrium is shifted toward the stable TlF adduct **1**, and no fluoride transfer takes place. Thus, the additional TlF inhibits the catalytic reaction, and only the stoichiometric reaction of Scheme 3 is possible.

Discussion

The Stabilization of 1: Steric Factors. There are both steric and electronic reasons that can explain why the reaction of [RuCl$_2$(PPh$_3$)$_3$] with Tl(I)F gives [Tl(μ-F)$_3$Ru(PPh$_3$)$_3$] instead of [RuF$_2$(PPh$_3$)$_3$] or [Ru$_2$(μ-F)$_3$(PPh$_3$)$_6$]$^+$. The small size of the fluoro ligand is obviously important to stabilize [Tl(μ-F)$_3$Ru(PPh$_3$)$_3$] as compared to [RuF$_2$(PPh$_3$)$_3$]. In the mixed-valence confacial bioctahedral complexes [Ru$_2$(μ-X)$_3$(tacn)$_2$] (X = Cl, Br, I; tacn = 1,4,7-triazacyclononane), the repulsive interactions between the halides in the bridge increase with increasing size of the halide (Cl < Br < I). However, the concomitant lengthening of the Ru−X bond limits the effect, and the X−Ru−X angle opens only slightly on going from Cl (88.8(14)°) to Br (90.0(9)°) and to I (90.9(2)°).[32]

With bulky phosphine ligands such as PPh$_3$ (or PCy$_3$), five-coordinate [RuX$_2$L$_3$] complexes are formed when X is Cl[33] (or Br). With smaller phosphines, the triply halide-bridged binuclear cations [L$_3$Ru(μ-X)$_3$RuL$_3$]$^+$ can be obtained instead.[34−36] As the structural effects of the halide in halo-bridged bioctahedral phosphine complexes of ruthenium(II) have not been systematically investigated, a homogeneous assessment is not possible. The F−Ru−F and P−Ru−P angles in **1** (76.0(3)° and 97.79(5)°, respectively) compare with the corresponding average values of [Ru$_2$(μ-F)$_3$(PEt$_3$)$_6$]$^+$ (73.7° and 95.8°).[16] In the chloro series, the Cl−Ru−Cl and P−Ru−P average values are 77.2° and 96.8° for [Ru$_2$(μ-Cl)$_3$(PEt$_2$Ph)$_6$]$^+$,[34a] 80.7° and 95.4° for [Ru$_2$(μ-Cl)$_3$(PMe)$_6$]$^+$,[34b] and 77.2° and 88.3° for [Ru$_2$(μ-Cl)$_3$((Ph$_2$PCH$_2$)$_3$CCH$_3$)$_2$]$^+$.[35] The iodo derivative [Ru$_2$(μ-I)$_3$(PMe$_2$Ph)$_6$]$^+$ has an average I−Ru−I angle of 80.0° and P−Ru−P angles in the range 92.2(4)−98.9(2)°.[36] These values confirm that the lengthen-

ing of the Ru−X bond down the halide series partially compensates the increase of the steric crowding with halide size on going from the (μ-F)$_3$ to the (μ-I)$_3$ bridge, so that the X−Ru−X angles remain nearly constant. Eventually, the phosphine−halide and phosphine−phosphine interactions are more important than those within the RuX_3Ru unit in determining the overall steric crowing in the complex.[30] Thus, the aggregation of two $[RuF_2(PPh_3)_3]$ units to form $[Ru_2(\mu\text{-}F)_3(PPh_3)_6]^+$, by analogy with $[Ru_2(\mu\text{-}F)_3(PEt_3)_6]^+$,[16] is probably disfavored by the interaction between the bulky PPh_3 ligands.

With bulkier donor sets than F_3P_3, even the coordination of the relatively small TlF to a five-coordinate fragment can be unfavorable. In fact, when a F_2P_4 donor set is present on ruthenium, the reaction of $[RuCl(P{-}P)_2]^+$ (P−P = diphosphine) with TlF yields the thallium adduct $[Tl(\mu\text{-}F)_2Ru(dppe)_2]^+$ with 1,2-bis(diphenylphosphino)ethane (dppe)[14] but the five-coordinate $[RuF(dppp)_2]^+$ in the case of the more bulky dppp ligand.[13] Thus, the formation of **1** instead of $[RuF_2(PPh_3)_3]$ is in line with the F_3P_3 donor set being overall less crowded than the F_2P_4 one.

The Stabilization of 1: Electronic Factors. Some halo complexes of late transition metals show surprising trends in a series of parameters (CO stretching frequencies, oxidation potentials, etc.) along the series F, Cl, Br, I, which suggest that the fluoro analogues are the most electron rich, although fluorine has the highest electronegativity.[1] This "inverse halide order" has been explained by postulating an exceptionally strong π-donation from the fluoro ligand,[6] which acts in combination with the 4-electron filled/filled pπ/dπ repulsions discussed by Mayer[7] and Caulton.[4] We have pointed out that there is consistent experimental evidence that the "inverse halide order" observed for d^6 and d^8 fluoro complexes is caused by the M−F bond having a higher ionic component than M−X bonds (X = Cl, Br, or I),[8] which is an effect of the high electronegativity of fluorine. Also, an analysis of the literature indicates that many d^6 and d^8 complexes with a terminal fluoro ligand either contain strong π-acidic ligands or are 16-electron, coordinatively unsaturated complexes, such as $[IrH_2F(PBu^t_2Ph)_2]$[12] and $[RuF(dppp)_2]^+$.[13] Thus, we have tentatively suggested that all factors that reduce the electronegativity difference between M and F favor the formation of fluoro complexes of d^6 and d^8 metals and lower the nucleophilic reactivity of the fluoro ligand.[8] We have argued, in terms of Pauling's electronegativity χ, that reducing the electronegativity difference $\Delta\chi$ between M and F decreases the ionicity and enhances the covalent character of the M−F bond.

However, we now notice that this conclusion contradicts the Pauling's central idea that the increasing polarity of a covalent bond reinforces the bond itself. In fact, the contradiction arises from the limited validity of Pauling's bond energy equation[45]

$$D^{o}_{AB} = \frac{1}{2}(D^{o}_{AA} + D^{o}_{BB}) + 23(\chi_A - \chi_B)^2$$

which holds for bonds where ($\chi_A - \chi_B$) is small, that is, for covalent bonds. Its validity decreases as the ionicity of the A−B bond increases, as Pearson[46] and Komorowski[47] have pointed out.

We suggest here a revision of our analysis of the M−F bond that overcomes the contradiction mentioned above by focusing on chemical hardness and the hard/soft acid/base (HSAB) principle[46,48] rather than on electronegativity. Parr and Pearson have defined chemical hardness of Lewis acids and bases as the average of the ionization potential I and electron affinity A[48]

$$\eta = (I - A)/2$$

and applied it to the HSAB principle.[48] The M−X bond formed in the reaction of the Lewis acid M^+ with the base X^-

$$M^+ + X^- \rightarrow M{-}X$$

has both a covalent and an ionic component. Thus, the (heterolytic) bond dissociation energy of the M−X bond can be decomposed into an ionic and a covalent component:

$$E = E(\text{ionic}) + E(\text{covalent})$$

The combination of a soft acid with a soft base gives a strong M−X bond in which the covalent component is the major one, and accounts for the bond strength. In hard/hard combinations, the electrostatic interactions result in a strong bond whose major component is the ionic one. A hard−soft (mismatched) adduct has a weak bond, as it is stabilized neither by the ionic component (weak charge transfer) nor by the covalent one (small orbital interactions).[48]

In the hypothesis that the hard/soft mismatch between F and M is responsible for the weakness of the M−F bond, and thus for the high nucleophilic reactivity of fluoro ligands in d^6 and d^8 complexes, then all factors that reduce the hard/soft mismatch between M and F are expected to strengthen the M−F bond. This can be achieved either by hardening M or by softening F. Before illustrating this line of reasoning with some examples, we point out the difference between this approach and our previous proposal.[8] Thus, the hardening of M strengthens the M−F bond because the ionic component of the bond becomes larger than in the hard/soft mismatched M−F, and not necessarily because the M−F bond becomes "more covalent" as we previously suggested.[8,49] However, one should appreciate that the hard/soft mismatch and the electronegativity difference between M and F are closely related, as electronegativity and hardness are roughly proportional.[48,50] Thus, any increase of electronegativity at the metal goes along with the "hardening" of M and the decrease of the M/F hard/soft mismatch.

(45) Pauling, L. *The Nature of the Chemical Bond*; Cornell University Press: Ithaca, NY, 1960; p 92.
(46) Pearson, R. G. *Chemical Hardness*; Wiley-VCH: Weinheim, 1997; p 24.
(47) Komorowski, L. *Struct. Bonding* **1993**, *80*, 45.
(48) (a) Parr, R. G.; Pearson, R. G. *J. Am. Chem. Soc.* **1983**, *105*, 7512. (b) Pearson, R. G. *Proc. Natl. Acad. Sci. U.S.A.* **1986**, *83*, 8440.
(49) We are grateful to Dr. Vladimir Grushin for bringing this point to our attention and for the enlightening discussions on this topic.

In the fluoro carbonyl complexes $[MF_2(CO)_2(PR_3)_2]$ (M = Ru or Os),[9a] the strong π-accepting CO ligands stabilize the dπ-orbitals of M, which increases the HOMO−LUMO gap in the $[M(CO)_2(PR_3)_2]^{2+}$ fragment. As the HOMO−LUMO gap is a rough estimate of the hardness of a molecule,[48b] its increase corresponds to the hardening of M, which strengthens the ionic component of the M−F bonds. Analogously, phosphine complexes of ruthenium(II) are soft and, in general, do not form complexes with neutral oxygen donors. However, phosphine complexes of ruthenium are oxophilic when containing hard coligands, such as imines or CO. The hardened ruthenium atom then forms aqua and triflato complexes, as in $[RuCl(OH_2)(PNNP)]^+$ (PNNP = *N*,*N*′-bis{(*o*-diphenylphosphino)benzylidene}-(1*S*,2*S*)-[diaminocyclohexane]),[51] $[RuCl_2(CO)(OH_2)(PEt_3)_2]$,[52] and $[Ru(O_3SCF_3)_2(OH_2)(CO)(dppe)]$.[53] The latter complex forms, in the presence of an excess of water, the extremely interesting species $[Ru(CO)(OH_2)_3(dppe)]^{2+}$, in which the strong π-accepting ligand and the double positive charge cooperate in enhancing the hardness of the metal, and hence its oxophilicity.

The hard/soft mismatch argument works equally well for the π-stabilized, 16-electron cations $[MFL_4]^+$ (M = d^6 ion; L = phosphine ligand). Let us consider $[MF_2L_4]$ and the corresponding fluoride dissociation product, the 16-electron species $[MFL_4]^+$. In fact, $[MFL_4]^+$ and $[MF_2L_4]$ derive from the acid−base reaction between fluoride and $[ML_4]^{2+}$ or $[ML_4]^+$, respectively. As any Lewis base (in this case fluoride) reduces the hardness of an ionic acid,[48a] the 16-electron complex $[MFL_4]^+$ is softer than the 14-electron $[ML_4]^{2+}$ fragment. Thus, the hard/soft mismatch between M and F is more severe in the neutral 18-electron complex $[MF_2L_4]$ than in the corresponding 16-electron cation $[MFL_4]^+$.

Besides the metal-based effects discussed above, the "hard/soft-mismatch" argument also explains ligand-based effects, and in particular the stability of the binuclear fluoro-bridged species of the type M−F−M′, such as $[Ru_2(\mu\text{-}F)_3(PEt_3)_6]^+$ (where M′ = $[Ru(PEt_3)_3]^{2+}$)[16] and **1**, **2**, and **3** (where M′ = Tl^+). Fluoride bridging between Ru and a soft acid M′ (Ru−F−M′) is a softer ligand than the terminal fluoro ligand (Ru−F) because of the symbiotic relationship of the former with M′ (a soft acid).[54] As both Ru(II) and Tl(I) are soft (η = 5.86 and 7.16 eV, respectively),[55a] this applies both to $[Ru_2(\mu\text{-}F)_3(PEt_3)_6]^+$, where M′ is $[Ru(PEt_3)_3]^{2+}$, and to **1**, where M′ is Tl^+.

The above considerations allow us to explain why **1** is formed instead of $[RuF_2(PPh_3)_3]$. As ruthenium(II) is soft (η = 5.86 eV) and F is hard (η = 7.01 eV),[55] the Ru−F bond in $[RuF_2(PPh_3)_3]$ will be weak. In the hypothetical reaction

$$[RuF_2(PPh_3)_3] + TlF \rightarrow [Tl(\mu\text{-}F)_3Ru(PPh_3)_3]$$

the soft thallium atom interacts with the hard F atoms of $[RuF_2(PPh_3)_3]$, and the soft ruthenium center with the hard F atom of TlF. On the basis of the principle of symbiosis,[54] these interactions harden ruthenium and soften fluoride in $[RuF_2(PPh_3)_3]$. As a result, the above reaction causes a decrease of the hard/soft mismatch between Ru and F in $[RuF_2(PPh_3)_3]$, and the Ru−F bond gets stronger.

A special case of bridging fluoride is given by the bifluoride anion FHF^-. Stable d^6 and d^8 bifluoride complexes have general formulas $[RuH_{2-n}(FHF)_nP_4]$ (n = 1 or 2),[56] $[PtH(FHF)P_2]$,[57] and $[Pd(FHF)(Ph)P_2]$.[58] These complexes, which exhibit Ru−F···F linkages with F···F distances in the range 2.28−2.40 Å and different degrees of bending,[58a] seem to contradict the principle of symbiosis, as both H^+ and HF are very hard.[55] However, there is an inverse relationship between hardness and molecular size[59] that allows one to predict that bifluoride FHF^- is softer than F^-. To put that on a quantitative basis, we estimated the hardness η of fluoride and bifluoride by using Pearson's operational definition of chemical hardness of anionic bases B^- as the average of the ionization potential I and electron affinity A of the corresponding radicals B·.[60,61] Thus, we calculated η of F· and FHF· from the corresponding ionizaton potentials (I) and electron affinities (A). The I and A values of the F· radical were calculated from the energies of F·, F^+, and F^- at the HF, MP2, and CCSD levels with the 6-31+G* basis set. The calculated I of F· (MP2, 17.08; CCSD, 17.01 eV) is underestimated but fairly close to the experimental value (17.42 eV) (Table 5).[48a] The calculated electron affinity is in excellent agreement with the experimental value (3.40 eV)[48a] for the MP2 model (3.40 eV), whereas the CCSD

(50) According to Mulliken and Jaffé, the electronegativity χ is defined as $\chi = (I + A)/2$. Both χ and η are dominated by the ionization potential I, which is the largest contribution to both of them. Thus, large η values parallel large χ values. See also: Huheey, J. E.; Keiter, E. A.; Keiter, R. L. *Inorganic Chemistry: Principles of Structure and Reactivity*; HarperCollins: New York, 1993.

(51) Stoop, R. M.; Bachmann, S.; Valentini, M.; Mezzetti, A. *Organometallics* **2000**, *19*, 4117.

(52) Sun, Y.; Taylor, N. J.; Carty, A. J. *Inorg. Chem.* **1993**, *32*, 4457.

(53) Mahon, M. F.; Whittlesey, M. K.; Wood, P. T. *Organometallics* **1999**, *18*, 4068.

(54) (a) Jørgensen, C. K. *Inorg. Chem.* **1964**, *3*, 1201. (b) For a quantomechanical interpretation, see: Nalewajski, R. F. *Struct. Bonding* **1993**, *80*, 117.

(55) (a) Pearson, R. G. *Inorg. Chem.* **1988**, *27*, 734. (b) The fact that Tl(I) is soft with η = 7.16 eV, yet F is hard with η = 7.01 eV, sounds confusing. However, it should be noted that, as the hardness scales for cations and anions span different ranges, the numerical values of η(anion) and η(cation) cannot be compared. Only comparison between anions or cations are meaningful: Tl(I) (η = 7.16 eV) is soft in comparison to Li^+ (η = 35.12 eV), and F^- (η = 7.16 eV) is hard in comparison to I^- (η = 3.70 eV).

(56) (a) Whittlesey, M. K.; Perutz, R. N.; Greener, B.; Moore, M. H. *Chem. Commun.* **1997**, 187. (b) Jasim, N. A.; Perutz, R. N.; Foxon, S. P.; Walton, P. H. *J. Chem. Soc., Dalton Trans.* **2001**, 1676. (c) Kirkham, M. S.; Mahon, M. F.; Whittlesey, M. K. *Chem. Commun.* **2001**, 813.

(57) (a) Jasim, N. A.; Perutz, R. N. *J. Am. Chem. Soc.* **2000**, *122*, 8685. (b) Hintermann, S.; Pregosin, P. S.; Rüegger, H.; Clark, H. C. *J. Organomet. Chem.* **1992**, *435*, 225.

(58) (a) Roe, D. C.; Marshall, W. J.; Davidson, F.; Soper, P. D.; Grushin, V. V. *Organometallics* **2000**, *19*, 4575. (b) Pilon, M. C.; Grushin, V. V. *Organometallics* **1998**, *17*, 1774. (c) Pilon, M. C.; Grushin, V. V. *J. Am. Chem. Soc.* **1998**, *119*, 44769.

(59) A general inverse relationship has been found between the global hardness of a molecule and molecular size (roughly estimated by the number of atoms in the molecule). See: Baekelandt, B. G.; Mortier, W. J.; Schoonheydt, R. A. *Struct. Bonding* **1993**, *80*, 211.

(60) Pearson, R. G. In *The Concept of the Chemical Bond*; Maksic, Z. B., Ed.; Springer: Berlin, 1990; p 46.

(61) Analogous calculations for open-shell radicals (including F·) have been reported: (a) Kar, T.; Scheiner, S.; Sannigrahi, A. B. *THEOCHEM* **1988**, *427*, 79. (b) Roy, R. K.; Pal, S. *J. Phys. Chem.* **1995**, *99*, 17822.

value (3.02 eV) is slightly underestimated. In sum, the experimental hardness of fluoride (7.01 eV)[48a] is fairly well reproduced by calculation (η = 6.84 (MP2) and 7.00 eV (CCSD)).

For the FHF· radical, the adiabatic ionization potential (I) and electron affinity (A) were calculated from the energies of FHF^-, FHF·, and FHF^+ after geometry optimization at the HF/6-31+G* and MP2/6-31+G* levels.[62] Vibrational analysis indicated that all the optimized structures correspond to energy minima. Both models (HF and MP2) gave analogous structures (Table 5). Bifluoride FHF^- has a linear, centrosymmetric structure ($D_{\infty h}$ symmetry), with a F···F distance of 2.268 (HF) and 2.329 Å (MP2), which is in good agreement with the experimental F···F distances in the range 2.26−2.40 Å.[63] The FHF· radical has $C_{\infty v}$ symmetry and can be described as F′−H···F·, with a large F···F separation and one short and one long H−F distance (Table 5). The FHF^+ cation is centrosymmetric ($D_{\infty h}$) with a F···F distance of 2.383 Å.

Energy calculations at the HF, MP2, and CCSD levels gave the energy values reported in Table 5. Although the calculated η values of FHF· vary depending on the model used, the qualitative trends of I and A show that the interaction with an HF molecule significantly increases the electron affinity of the F· radical and reduces its ionization potential. The sum of these two effects is a decrease of the hardness of fluoride upon interaction with HF. The η values indicate that bifluoride (FHF^-) is less hard (η = 4.04−5.20 eV) than fluoride (η_{exp} = 7.01 eV). This is in agreement with qualitative arguments based on molecular size[59] and, more importantly, with chemical evidence, that is, the formation of bifluoride complexes instead of the corresponding species containing terminal fluoro ligands.[56−58] Thus, the bridging coordination mode (M−F−M′) softens fluoride even when a hard partner (M′) such as HF is involved.

Interestingly, there is a parallel between fluoride and other hard, π-donor ligands, such as oxo, hydroxo, and amido, which tend to prefer the bridging coordination mode when bound to soft late transition metals in low oxidation states. Mayer has attributed this preference to the redistribution of the 4-electron filled/filled pπ/dπ repulsion over several centers.[7] Holland, Andersen, and Bergman have criticized this approach and argued that, as the stabilization energy from π-bonding between M and N in alkylamide complexes of early transition metals is estimated to be less than 10 kcal/mol, the corresponding 4-electron pπ/dπ repulsion energy would be small (probably not more than 1−2 kcal/mol).[17] They suggested an alternative analysis of alkoxo and amido cyclopentadienyl Ni complexes that focuses on the ionic character of the M−X bond rather than on π-effects, which is analogous to our analysis of the M−F bond. Application of Drago's *E-C* theory[64] to thermochemical data of cyclopentadienyl Ni complexes indicates that the ionic component of the M−X bond dominates over the covalent one and determines the thermodynamic preferences of M toward N or O donors.[17]

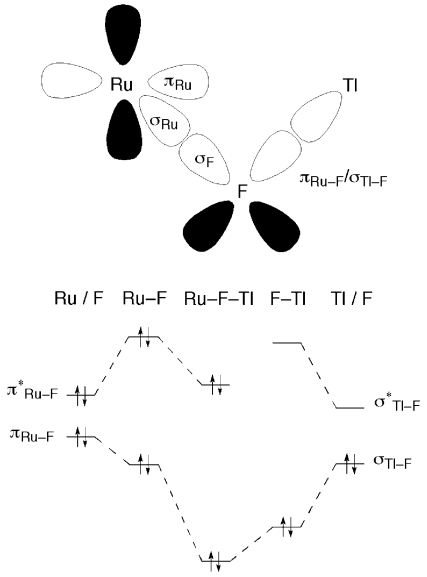

Figure 8. Schematic orbital description of the Ru−F−Tl bond in **1**.

A final remark is that the explanation of the electronic factors across the Ru−F−M bridge in terms of π-effects is inconsistent with experiment, which indirectly reinforces the hard/soft-mismatch argument exposed above. As sketched in Figure 8, the doubly occupied Ru and F orbitals with π-symmetry (Ru/F) give rise to a 4e-interaction (Ru−F). The Tl atom involves the p(F)-orbitals with Ru−F π-character (π_{Ru-F}) in a partially covalent dative Tl−F σ-bond (σ_{Tl-F}) and lowers their energy (F−Tl). This is expected to relieve the filled/filled interaction between F and Ru, that is, to lower the energy of the π^*_{Ru-F} orbital (Ru−F−Tl). Clearly, the same consideration applies to $[Ru_2(\mu\text{-}F)_3(PEt_3)_6]^+$, which can be formally considered as formed by a "$[P_3RuF_3]^-$" fragment interacting with a "$[RuP_3]^{2+}$" dication. However, the Ru−F distances in the latter species (in the range 2.132(2)−2.170(2) Å) and in **1** (2.133(3) Å) are very similar, which suggests that Tl^+ and "$[RuP_3]^{2+}$" cause similar effects upon coordination onto "$[P_3RuF_3]^-$". This observation suggests that there is no significant destabilization that can be ascribed to pπ/dπ filled/filled interactions, which should be operative in $[Ru_2(\mu\text{-}F)_3(PEt_3)_6]^+$ but not in **1**.

Final Remarks

We have recently discussed the effect of the ionic nature of the M−F bond in d^6 and d^8 complexes and described some metal-based features that stabilize low-valent fluoro complexes of late transition metals.[8] These features are the presence of strong π-acceptor ligand that gives a push−pull-interaction[4] with F or the electron deficiency of the π-stabilized[11] cationic complexes $[MXL_4]^+$. We agree with Perutz's statement that the bridging mode favors the coordination of fluoride to late transition metal ions.[16] Therefore, we suggested here a unified vision of the coordination modes of fluoride (terminal or bridging) in terms of the HSAB

(62) MP2 calculations have been reported to account satisfactorily for electron correlation in bifluoride: Kawahara, S.; Uchimaru, T.; Taira, K. *Chem. Phys.* **2001**, *273*, 207.
(63) See refs 6−25 in ref 23.
(64) Drago, R. S. *Applications of Electrostatic-Covalent Models in Chemistry*; Surfside: Gainesville, FL, 1994.

model. As for the bridging coordination mode, we notice that additional covalent interactions "soften" the fluoro ligand and reduce thereby the hard/soft mismatch between Ru and F. The latter effect strengthens the covalent component of the Ru−F bond in the Ru−F-M′ unit and stabilizes d^6 complexes containing bridging fluoro ligands. This explanation can be reversed to explain the metal-based effects mentioned above. In fact, push−pull interactions and electron deficiency "harden" the metal and strengthen the M−F bond by means of its ionic component in complexes that either contain strong π-accepting ligands or are 16-electron cations.

Supporting Information Available: Listings of X-ray data of **1**, **2**, and **3** (atomic coordinates, anisotropic thermal parameters, bond distances and angles, and calculated positions of H atoms) (CIF format), as well as the ^{31}P and ^{19}F NMR spectra of **1** (S1) and the ^{31}P NMR spectrum of **3** (S2). This material is available free of charge via the Internet at http://pubs.acs.org.

IC034888E